AIAA 82-4159

Finite Element Solution of Heat Transfer for Gas Flow through a Tube

Muhammad M. Razzaque,* John R. Howell,† and Dale E. Klein‡
The University of Texas at Austin, Austin, Texas

An analysis was performed of the axial temperature distribution along the wall of a circular tube. A transparent gas in forced convection enters a tube with variable heat-transfer coefficient, internal radiation exchange, and axial wall heat conduction. The nonlinear integro-differential equation describing the process of energy exchange was solved using the Galerkin finite element technique with isoparametric, quadratic elements. An arbitrary heat generation distribution in the tube wall as a function of axial position can be taken into this model, depending on the particular physical problem; however, only the uniform and the sinusoidal heat generation cases have been considered here. The tube interior surface was assumed to be black, and the gas was considered transparent. This type of problem is of practical interest for the high-temperature, gas-cooled reactor (HTGR) core flow and for tubular heat-exchanger flow. In an HTGR the coolant is helium and can be well approximated as a transparent gas. Similar problems also arise for flow of a gas through electrically heated tubes and coils. Results for only the uniform heat generation case are available from other numerical techniques, and the results using the finite element method were found to be in good agreement.

Nomenclature

C_p = specific heat at constant pressure, J/kg°C
D = tube diameter, m
h = convective heat-transfer coefficient, W/m²°C
h_∞ = fully developed convective heat-transfer coefficient, W/m²°C
k = thermal conductivity, W/m°C
L = tube length, m
q = heat added at wall per unit inside area and time, W/m²
R = tube radius, m
T = temperature, °C
$\bar{u}$ = mean gas velocity, m/s
X,Z = axial length coordinates measured from the tube entrance, m
ρ = density of gas, kg/m³
σ = Stefan-Boltzmann constant, W/m²K⁴

Dimensionless Parameters

F = geometric configuration factor between differential ring element and circular plane at tube end opening
H = convective heat-transfer coefficient = $(h/q)\,(q/\sigma)^{1/4}$
H_∞ = fully developed heat-transfer coefficient = $(h_\infty/q)\,(q/\sigma)^{1/4}$
Kdz = geometric configuration factor between differential ring elements on inside of tube
ℓ = length = L/D_i
p = conduction parameter = $(k_w/4qD_i)\,[(D_o/D_i)^2-1](q/\sigma)^{1/4}$
S = Stanton number = $4h_\infty/\bar{u}\rho C_p$
t = temperature = $(\sigma/q)\,T^{1/4}$
x = coordinate = X/D_i
y = dummy integration variable
z = length = Z/D_i
δ = numerical constant

Subscripts

g = gas
i = inner dimension of tube
o = outer dimension of tube
w = wall
X,Z = position along tube length
1 = inlet end of tube
2 = exit end of tube

Introduction

ANALYTICAL solutions to engineering heat transfer problems involving radiant energy interchange have proved mathematically formidable owing to the nonlinear mechanism of the radiation processes, geometric complexities, and simultaneous interaction of all parts of the participating continuum. In this study a finite element method (FEM) is used to develop a model of radiation coupled with conductive and convective modes to provide an accurate solution in determining the temperature profile along a circular tube. The FEM is sufficiently general to treat variations in geometry, boundary conditions, and the parameters involved in the problem, such as externally imposed heat flux, heat transfer coefficient, tube wall emissivity, etc.

The result for the case of uniform externally imposed heat flux was solved by earlier investigators before the common utilization of high-speed computers is shown in Ref. 1. For one set of parameters and for five ring-area intervals on the tube wall, the solution required 10 h of hand computation.

Table 1 Comparison of dimensionless wall temperature distribution for uniform heat flux with that of Ref. 2[a]

x	Finite element method	Other numerical method[2]
0	1.85	1.80
2.5	2.04	2.05
5	2.13	2.14
7.5	2.09	2.10
10	1.94	1.94

[a] $p=10$, $H=H_\infty\{1+[1/2(x+\delta)^{5/6}]\}$, where $H_\infty=0.8$, $\delta=0.01$, $t_1=t_{g,1}=1.5$, $t_2=t_{g,2}$, $S=0.01$, $\ell=10$.

Received April 20, 1981; revision received Oct. 30, 1981.

*Engineer, Nuclear Fuel Resources Department, Virginia Electric and Power Company, Richmond, Va.
†Professor, Department of Mechanical Engineering. Associate Fellow AIAA.
‡Assistant Professor, Department of Mechanical Engineering.

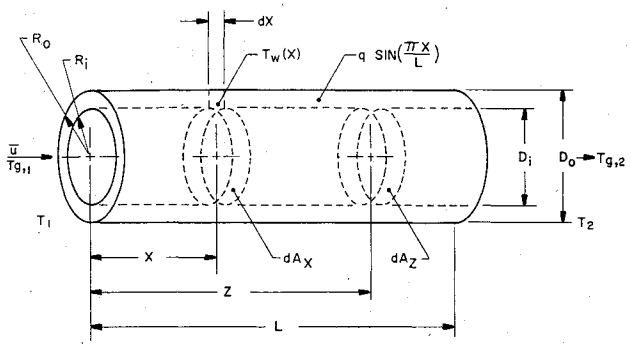

Fig. 1 Cylindrical tube geometry.

This example illustrates the complexities arising in such problems. Siegel and Keshock[2] employed a finite difference method to solve the problem with constant wall heat flux. They used a special technique to treat the integral term in the energy balance equation to achieve convergence. The results are compared with those of FEM in Table 1. Application of FEM to solve integral equations has been discussed in Refs. 3 and 4. However, the finite element solution of the type of combined-mode heat-transfer problem discussed in this paper, which gives rise to highly nonlinear integro-differential equations, has not been attempted earlier.

In many practical situations, the externally imposed heat flux is not uniform, but is rather some function of channel axial position. If the functional dependence of the wall heat flux is known, it can be used directly in the FEM model. For illustration and also because of its applicability in nuclear reactors, a sinusoidal heat flux distribution has also been considered in the present analysis. The resulting wall and gas temperature profiles are shown.

Analysis

A circular flow channel with a specified heat flux is cooled by a gas that does not absorb, emit, or scatter radiation, as shown in Fig. 1. The gas enters the tube at temperature $T_{g,1}$ from a chamber at T_1 and it leaves the tube at $T_{g,2}$ and enters a mixing plenum that is at temperature T_2. The tube interior surface is considered black and the exterior surface is perfectly insulated. For a differential element on the tube surface (see Fig. 1), the energy balance can be formed as

$$\frac{k_w(R_o^2-R_i^2)}{2R_i}\left(\frac{d^2T_w}{dX^2}\right)+q\sin\left(\frac{\pi X}{L}\right)+q_i = q_o+h(X)[T_w(X)-T_g(X)] \tag{1}$$

The terms on the left of Eq. (1) include the externally imposed sinusoidal heat input and the incoming radiation, q_i. On the right of Eq. (1) is the outgoing radiation, q_o, and the heat leaving by convection from the wall to the gas. The term q_o is composed of direct emission and is given by

$$q_o=\sigma T_w^4 \tag{2}$$

The term q_i is composed of two components, the radiation coming from the reservoirs at the ends of the tube and the radiation arriving as a result of the outgoing energy from the other elements on the internal tube surface. These quantities can be written as

$$q_i=\sigma T_1^4F(X)+\sigma T_2^4F(L-X)+\int_0^L q_o(Z)K(|X-Z|)dZ \tag{3}$$

The function $F(X)$ is the geometric configuration factor for radiation from an element on the tube wall at location X to the circular opening at the inlet end of the tube. This factor is given by

$$F(x)=\frac{x^2+\frac{1}{2}}{(x^2+1)^{\frac{1}{2}}}-x \qquad x\geq 0 \tag{4}$$

where $x=X/D_i$.

The reservoirs are assumed to be represented by black circular disks at the end openings of the tube. The function $K(a)dz$ is the configuration factor between two differential rings a distance a apart on the inside surface of the tube and is given by

$$K(a)dz=1-\frac{a^3+3a/2}{(a^2+1)^{3/2}}dz \qquad a\geq 0 \tag{5}$$

where $a=(Z-X)/D_i$, and $z=Z/D_i$.

Substituting Eqs. (2) and (3) into Eq. (1) and making them dimensionless results in the following expression:

$$p\left(\frac{d^2t_w}{dx^2}\right)+\sin\frac{\pi x}{\ell}+\int_0^{\ell}t_w^4(z)K(|x-z|)dz+t_1^4F(x) +t_2^4F(\ell-x)=t_w^4(x)+H(x)[t_w(x)-t_g(x)] \tag{6}$$

where $\ell=L/D_i$.

An additional heat balance is written for the flowing gas to relate T_w and T_g. Since the gas is transparent to radiation, the only heat transfer to the gas is by convection from the wall. For a cylindrical volume element of length dX and diameter D_i, the rate of heat transfer can be represented as

$$h(X)\pi D_i dX[T_w(X)-T_g(X)]$$

This is equal to the net heat carried out of the volume element by the flowing gas, which can be represented as

$$\bar{u}\left(\frac{\pi D_i^2}{4}\right)\rho C_p\left(\frac{dT_g}{dX}\right)dX$$

These two quantities can be equated and made dimensionless to form the following equation:

$$\frac{dt_g(x)}{dx}=S\frac{H(x)}{H_\infty}[t_w(x)-t_g(x)] \tag{7}$$

Equations (6) and (7) are two coupled, nonlinear integro-differential equations to be solved with the following boundary conditions. The end edges of the tube are insulated so that, for Eq. (6),

$$\frac{dt_w}{dx}=0 \qquad \text{at} \quad x=0 \text{ and } x=\ell$$

and for Eq. (7),

$$t_g=t_{g,1} \qquad \text{at} \quad x=0$$

where $t_{g,1}$ is a known value.

It is pointed out in Refs. 5 and 6 that for sinusoidal heat generation, a constant heat-transfer coefficient is a reasonably good approximation and for uniform heat generation, a heat-transfer coefficient has been taken to be of the form as given in Ref. 2:

$$H(x)=H_\infty\left[1+\frac{1}{2(x+\delta)^{5/6}}\right] \tag{8}$$

where $\delta=0.01$.

Substituting Eq. (8) into Eq. (7) and solving the first-order differential equation for the gas temperature in terms of the wall temperature gives the following equation:

$$t_g(x) = S\ \exp(-S\{x+3[(x+\delta)^{1/6}-\delta^{1/6}]\})$$
$$\times \int_0^x \exp(S\{y+3[(y+\delta)^{1/6}-\delta^{1/6}]\})\left[1+\frac{1}{2(y+\delta)^{5/6}}\right]$$
$$\times t_w(y)\,dy + t_{g,1}\exp(-S\{x+3[(x+\delta)^{1/6}-\delta^{1/6}]\}) \quad (9)$$

For purely computational advantage, which will be discussed later in the Results and Discussion section, $t_w = u^{1/4}$ was substituted in Eq. (6), and the equation was rearranged to obtain

$$-\frac{p}{4u^{3/4}}\left(\frac{d^2u}{dx^2}\right)+u=\sin\left(\frac{\pi x}{\ell}\right)-\frac{3p}{16u^{7/4}}\left(\frac{du}{dx}\right)^2-H(x)u^{1/4}$$
$$+H(x)t_g(x)+\int_0^\ell u(y)K(|x-y|)dy+t_1^4F(x)+t_2^4F(\ell-x) \quad (10)$$

Finally, substituting Eq. (9) into Eq. (10) one can get a single equation with only one unknown, u.

$$-\frac{p}{4u^{3/4}}\left(\frac{d^2u}{dx^2}\right)+u=\sin\left(\frac{\pi x}{\ell}\right)-\frac{3p}{16u^{7/4}}\left(\frac{du}{dx}\right)^2-H(x)u^{1/4}$$
$$+t_1^4F(x)+t_2^4F(\ell-x)+H_\infty t_{g,1}$$
$$\times\exp(-S\{x+3[(x+\delta)^{1/6}-\delta^{1/6}]\})$$
$$\times\left[1+\frac{1}{2(x+\delta)^{5/6}}\right]+SH_\infty\left[1+\frac{1}{2(x+\delta)^{5/6}}\right]\exp(-S\{x+3$$
$$\times[(x+\delta)^{1/6}-\delta^{1/6}]\})\int_0^x\exp(S\{y+3[(y+\delta)^{1/6}-\delta^{1/6}]\})$$
$$\times\left[1+\frac{1}{2(y+\delta)^{5/6}}\right]u^{1/4}dy+\int_0^\ell u(y)K(|x-y|)dy \quad (11a)$$

The boundary conditions are

$$\frac{du}{dx}=0 \text{ at } x=0 \text{ and } x=\ell \quad (11b)$$

The notation in Eq. (11a) is simplified by letting the right-hand side be equal to $f(x,u)$ and $A(u)=p/(4u^{3/4})$. Equation (11a) then becomes

$$-\frac{d}{dx}\left[A(u)\frac{du}{dx}\right]+u=f(x,u) \qquad 0<x<\ell \quad (12)$$

with the boundary condition still given by Eq. (11b).

Galerkin Finite Element Formulation

It is not the intention of this paper to go into details of the finite element method (FEM). Rather, the basic concept of the method and its direct application of the problem at hand are outlined. For details of the method the reader is referred to an excellent text (to be published) by Becker, Carey, and Oden[7] and texts published by Zienkiewicz[8] and Heubner.[9]

The weak (or variational) statement of Eq. (12) is given as follows: find the function u such that all weighted averages of the differential equation, together with the boundary conditions, are satisfied. By a "weighted average" of the differential equation, it is required that

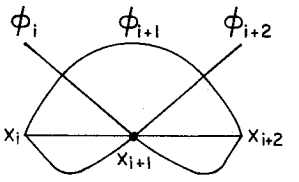

Fig. 2 Quadratic shape function on an element in x coordinate.

$$\int_0^\ell\left[-\frac{d}{dx}\left[A(u)\frac{du}{dx}\right]+u\right]V dx-\int_0^\ell f(x,u)\,V dx=0 \quad (13)$$

for all members of V of a suitable class of functions. In Eq. (13) the "weight function," or "test function," V, is any function of x that is sufficiently well behaved that the integrals are meaningful. Integrating the first term of Eq. (13) using integration-by-parts and introducing the boundary values gives the following equation:

$$\int_0^\ell\left[A(u)\frac{du}{dx}\frac{dV}{dx}+uV\right]dx-\int_0^\ell f(x,u)\,V dx=0 \quad (14)$$

We now seek an approximate solution $U(x)$ of the form

$$u(x)\approx U(x)=\sum_{j=1}^N \alpha_j\phi_j(x) \quad (15)$$

and assume the form of the test function as

$$V(x)=\sum_{i=1}^N \beta_i\phi_i(x) \quad (16)$$

where α_j and β_i are constant coefficients and $\phi(x)$ is called a "shape function." A typical quadratic shape function on the x coordinate is shown in Fig. 2. Introducing Eqs. (15) and (16) into Eq. (14) and rearranging gives

$$\sum_{i=1}^N \beta_i\left(\sum_{j=1}^N\left\{\int_0^\ell\left[A(U)\frac{d\phi_i}{dx}\frac{d\phi_j}{dx}+\phi_i\phi_j\right]dx\right\}\alpha_j\right.$$
$$\left.-\int_0^\ell f(x,U)\phi_i dx\right)=0 \quad (17)$$

for all β_i.

One can rewrite Eq. (17) in a more compact form as

$$\sum_{i=1}^N \beta_i\left[\sum_{j=1}^N K_{ij}\alpha_j-f_i\right]=0 \quad (18)$$

for all β_i, where

$$K_{ij}=\int_0^\ell\left[A(U)\frac{d\phi_i}{dx}\frac{d\phi_j}{dx}+\phi_i\phi_j\right]dx \quad (19)$$

and

$$f_i=\int_0^\ell f(x,U)\phi_i dx \qquad i,j=1,2,\ldots,N \quad (20)$$

The matrix K_{ij} is called the "stiffness matrix," and the vector f_i is sometimes known as a "load vector."

Because the β_i are arbitrary, Eq. (18) represents N equations to be satisfied by the α_j rather than the single equation it may appear to be. Thus we arrive at the system of N nonlinear algebraic equations in the N unknown coef-

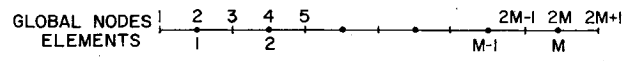

Fig. 3 Finite element mesh.

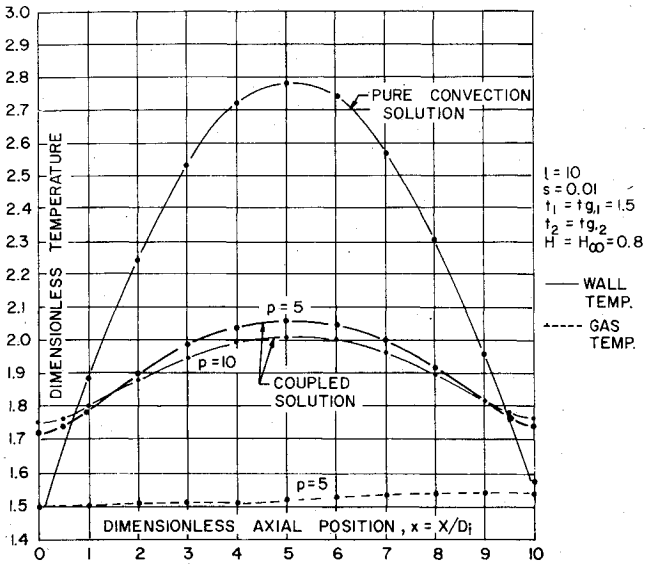

Fig. 4 Comparison of solutions to illustrate effects of radiation and axial wall conduction with sinusoidal heat flux for tube $\ell = 10$.

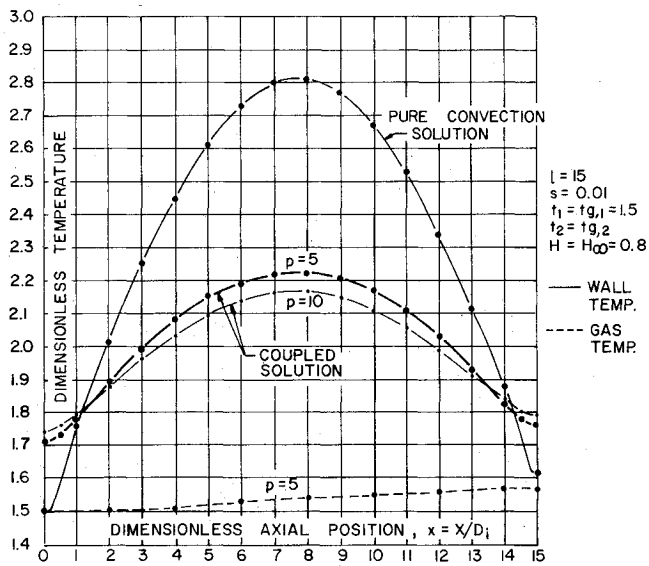

Fig. 5 Comparison of solutions to illustrate effects of radiation and axial wall conduction with sinusoidal heat flux for tube $\ell = 15$.

ficients α_j:

$$\sum_{j=1}^{N} K_{ij}\alpha_j = f_i \qquad i = 1,2,\ldots,N \tag{21}$$

The shape functions are chosen in such a way that the parameters α_j defining the approximating solution $U(x)$ are precisely the value of $U(x)$ at the nodal points in the finite element mesh. If the shape functions are defined on each of the nodes of an element only, the element is called an isoparametric element.

To carry out the process computationally, first the system domain is subdivided into a finite number of subdomains called "finite elements" and then an appropriate shape function is chosen. The integration in Eqs. (19) and (20) are

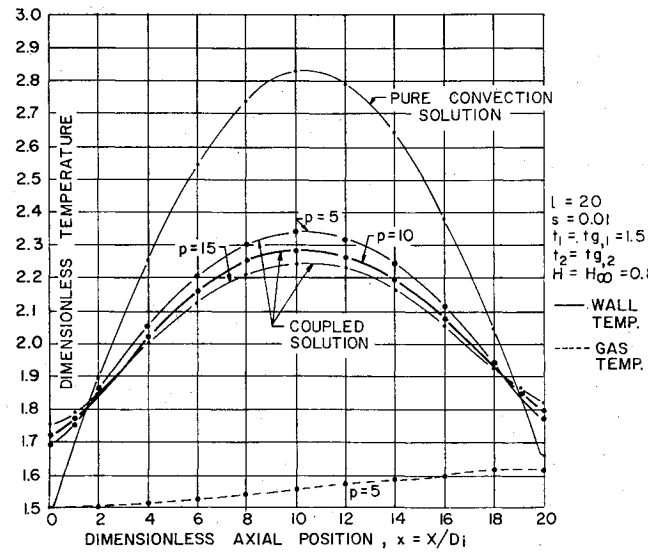

Fig. 6 Comparison of solutions to illustrate effects of radiation and axial wall conduction with sinusoidal heat flux for tube $\ell = 20$.

carried out numerically piecewise on each element to compute the elemental stiffness matrix and load vector, respectively. Finally, the elemental stiffness matrices and load vectors are assembled in a proper fashion to form the global stiffness matrix K_{ij} and load vector f_i, respectively, as required by Eq. (21) to solve for the unknown vector α_j.

In the present analysis, the system domain was subdivided into isoparametric, quadratic elements having three degrees of freedom (or nodes) per element, as shown in Fig. 3. The shape function was chosen to be quadratic, as shown in Fig. 2. The numerical integration was performed using a fourth order Gaussian quadrature integration scheme. Nonlinearity enters into the problem due to the fact that both the stiffness matrix and the load vector are functions of the unknown, which in the present problem is the fourth power of the tube wall temperature. Therefore, the matrix Eq. (21) has to be solved by an iterative technique. The first iteration was started with guessed values of the wall temperature at each node, and the solution vector was used to continue the next iteration until convergence was achieved. Once the wall temperature is known, the gas temperature can be evaluated easily using Eq. (9).

Results and Discussion

The dimensionless tube wall temperature distribution obtained for the case of uniform heat generation is compared with published data[2] in Table 1 and found to be in good agreement. The analysis went further to include sinusoidal heat generation in the tube wall as a means to demonstrate that any functional dependence of axial heat flux distribution can be included easily into this model. These results of wall and gas temperature distribution with combined modes of conduction, convection, and radiation together with a pure convection limit are shown in Fig. 4, 5, and 6 for tube length-to-diameter ratios of 10, 15, and 20, respectively.

For the parameters chosen in this analysis and with $p = 10$, the peak wall temperatures are lower with combined modes than pure convection by 28% for a 10 diameter long tube, 23% for a 15 diameter long tube, and 19% for a 20 diameter long tube. Therefore it is evident that for relatively short tubes the effect of radiation and conduction on wall temperature is significant. It is also evident from the analysis that as the tube length-to-diameter ratio is increased, the effect of radiation and conduction on the tube wall temperature distribution diminishes, and convection becomes the more dominant mode of heat transfer.

The effectiveness of axial wall conduction depends also on the dimensionless conduction parameter p. For high-temperature materials and typical heat-exchanger tube wall thicknesses, p is generally below 10, especially if the wall heat flux is high. For this range of p, the influence of conduction was found to be relatively low. However, for heat-exchanger elements, electrically heated tubes and coils, or similar instances where the length-to-diameter ratio is comparatively small, neglecting the effect of radiation may introduce considerable error in calculating the gas or wall temperature. For the case of a graphite core flow channel in a high-temperature, gas-cooled reactor (HTGR), the value of p is normally less than 10 because of the high core heat flux, and the coolant flow channel is about 300 diameters long. Due to the very long channel length and lower value of p, a pure convection limit can serve as a good approximation in calculating axial wall temperature in the HTGR core. The physical explanation of such an observation is based on the fact that for a long channel with a large length-to-diameter ratio, less energy can radiate through the end openings. In addition, as a result of the long conduction path, heat loss by conduction is lower in such a situation. Thus the chief mechanism of heat transfer in a long channel is convection.

A few comments are in order concerning the finite element numerical technique. The equation for pure radiation is linear in the fourth power of the wall temperature. However, when radiation is coupled with conduction and/or convection, the resulting equation becomes nonlinear because both conduction and convection are functions of the wall temperature. This nonlinearity introduces an integral term with a fourth power of wall temperature in the load vector which tends to diverge rapidly if the initial guess is not close to the true solution. To overcome this difficulty, a new dependent variable of $u=t_w^4$ was substituted into the coupled equation. The equation was then rearranged in the manner as shown in Eq. (10) (that is, to keep the second derivative term and the term with the first power of the new dependent variable on the left side of the equation and the rest of the terms on the right side of the equation) to be able to generate a symmetric stiffness matrix.

This method saved considerable computer memory storage. For tube length-to-diameter ratios of 10, 15, and 20, reasonably good results were obtained by using 20, 30, and 40 elements, respectively. Doubling the number of elements makes about a 1% change in the result, whereas the computer time increases by a factor of 3. Likewise, as the tube length-to-diameter ratio is increased, more elements are required to obtain acceptable results, a situation that in turn raises the computer time requirement rather sharply.

Another parameter whose magnitude affects the computer time requirement is the conduction parameter p. For $p>15$, the number of iterations needed for convergence was smaller and, therefore, the computer time requirement was less. Of course, in order to know the exact number of iterations, one needs to know values of the other parameters in Eq. (11) as well. Conversely, for $p<5$, the number of iterations needed was larger and, hence, required a longer computer time. As $p\to 0$, convergence could not be achieved in general.

The direct iteration method with an overrelaxation factor of 1.8 was used to achieve convergence with a minimum number of iterations. It was noted in this study that to achieve convergence and to get an accurate solution, one needs to evaluate the integrals on the right-hand side of Eq. (11) very accurately. FEM provides a definite advantage over other numerical methods in this respect because the shape functions, being curvilinear and continuous over the whole domain, allow the integrals to be evaluated accurately.

Concluding Remarks

The purpose of the present analysis is to demonstrate that the finite element method (FEM) is a viable numerical technique to solve the type of heat-transfer problem discussed in this paper. A few specific practical applications are discussed. It is found not only that the FEM is a viable method to solve the nonlinear integro-differential equation that arises in combined-mode heat-transfer problems, but that it has the following additional advantages:

1) The model can include flow channels of other geometries than a circular tube as long as the descriptive mathematical equations can be developed.

2) Any functional dependence of axial heat flux distribution can be included in the model.

3) Variation in the parameters taken in this study, such as externally imposed heat flux, heat transfer coefficient, tube wall emissivity, etc., can be handled by the model.

4) Higher-order approximations of the temperature distribution can be attained by using higher-order shape functions.

5) FEM computer codes are generally easy to use because they allow variation in geometry, material properties, and boundary conditions of the system in question by changing a minimal number of input data.

References

[1] Siegel, R. and Howell, J. R., *Thermal Radiation Heat Transfer*, 2nd ed., McGraw-Hill Book Co., New York, 1981, p. 403.

[2] Siegel, R. and Keshock, E. G., "Wall Temperatures in a Tube with Forced Convection, Internal Radiation Exchange, and Axial Wall Heat Conduction," NASA TN D-2116, March 1964.

[3] Wong, J. P. and Aguirre-Ramirez, G., "Numerical Solution of Integral Equations by Finite Element Method," *Proceedings of the 12th Annual Meeting*, Society of Engineering Science, 1975, pp. 981-988.

[4] Reddy, J. N. and Murty, V. D., "Finite-Element Solution of Integral Equations Arising in Radiative Heat Transfer and Laminar Boundary-Layer Theory," *Numerical Heat Transfer*, Vol. 1, 1978, pp. 389-401.

[5] Shenoy, A. S. and McEachern, D. W., "HTGR Core Thermal Design Methods and Analysis," General Atomic Company, San Diego, Calif., GA-A12985, Dec. 1974.

[6] Siegel, R., "Combined Radiation and Forced Convection for Flow of a Transparent Gas in a Tube with Sinusoidal Axial Wall Heat Flux Distribution," NASA TN D-1441, Oct. 1962.

[7] Becker, E. B., Carey, G. F., and Oden, J. T., *Finite Elements: An Introduction* (Vol. I in a series of texts and monographs to be published by Prentice-Hall Publishing Co., Englewood Cliffs, N. J.).

[8] Zienkiewicz, O. C., *The Finite Element Method*, 3rd ed., McGraw-Hill Book Co., New York, 1977.

[9] Heubner, K. H., *The Finite Element Method for Engineers*, John Wiley and Sons, New York, 1975.